

A study case on the upscaling of tree transpiration in Water Limited Environments

Andrea I. Salinas Revollo
March, 2010

Course Title: Geo-Information Science and Earth Observation
for Environmental Modelling and Management

Level: Master of Science

Course Duration: September 2008 - March 2010

Consortium partners: University of Southampton
Lund University (Sweden)
University of Warsaw (Poland)
International Institute for Geo-Information Science
and Earth Observation

GEM thesis number: 2010-24

A case study on the upscaling of tree transpiration in Water Limited Environments

by

Andrea I. Salinas Revollo

Thesis submitted to the International Institute for Geo-information Science and Earth Observation in partial fulfilment of the requirements for the degree of Master of Science in Geo-information Science and Earth Observation for Environmental Modelling and Management

Thesis Assessment Board

Chairman	Dr. Ir. C.M.M. Mannaerts, Associate Professor, ITC
First Supervisor	M.Sc. Valentijn Venus, Lecturer, ITC
Second Supervisor	Dr. Ir. M.W. Lubczynski, Associate Professor, ITC
External Examiner	Dr. Petter Pilesjö, Associate Professor, Lund University
Advisor	MSc. Leonardo Reyes, PhD candidate, ITC



UNIVERSITY OF TWENTE.

ITC

FACULTY OF GEO-INFORMATION SCIENCE AND EARTH OBSERVATION

Disclaimer

This document describes work undertaken as part of a programme of study at the International Institute for Geo-information Science and Earth Observation. All views and opinions expressed therein remain the sole responsibility of the author, and do not necessarily represent those of the institute.

Abstract

Direct methods are effective for estimating transpiration in areas where the water balance and vegetation characteristics are highly variable. Usually, transpiration is calculated as a component of catchment evapotranspiration in spatial modelling of water resources. This leads to uncertainty about the actual values of plant transpiration and soil evaporation. Nevertheless, this information is important for conservation and planning in sub-humid and arid areas where vegetation can take up a significant amount of water. In this study, transpiration was directly estimated, based on data from a sap flow and leaf ecophysiology measurement campaign conducted in north-western Spain, in a semi-arid catchment where *Quercus Ilex* and *Quercus Pyrenaica* are the dominant species. Estimations obtained with the Penman-Monteith model were compared with sap flow transpiration estimations at the tree, stand and catchment levels.

In order to identify tree species throughout the catchment, two methods of classification were performed on a Quickbird satellite image. A procedure based on supervised classification and object-oriented analysis proved to have greater accuracy (0.80 overall accuracy, Kappa = 0.31, true accuracy between 0.75 and 0.84 at p 0.05) than a multi-criteria method using GIS (0.79 overall accuracy, Kappa = 0.23, true accuracy between 0.74 and 0.83 at p 0.05).

Sap flow measurements were scaled up using sapwood area and canopy area, while Penman-Monteith estimates were scaled up using Leaf Area Index (LAI) and the fraction of sunlit and shaded parts of the canopy. At the tree level, Penman-Monteith estimations were closer to sap flow estimations when LAI was applied using a “big leaf” model (RMSE = 296.2 cm³/h for *Q. Pyrenaica* and 542.6 cm³/h for *Q. Ilex*, as compared with sap flow values) than using a simple 4-layer representation of the canopy (RMSE = 430.2 cm³/h for *Q. Pyrenaica* and 8543.9 cm³/h for *Q. Ilex*). For a 1 Ha stand with 19 trees, the estimated transpiration was 0.148 m³/h with sap flow measurements, and 0.138 m³/h with the Penman-Monteith model. Finally, at the catchment level, the sap flow estimation of transpiration was 4.94 m³/h and 11.92 m³/h with the Penman-Monteith model. Differences arise mainly from the assumptions and generalizations taken for both estimations.

It is concluded that simple, direct methods (e.g. sap flow measurements, “big leaf” upscaling procedures) are effective for transpiration estimation, but the generalizations and assumptions associated with them are an obstacle for validation.

Acknowledgements

In the following lines I would like to express my sincere appreciation to all the persons that have made the publication of this work possible.

First, a great “thank you” to my supervisor Valentijn Venus, for being always available, have lots of patience, give support in the last difficult moments and for playing Keane during fieldwork...

Also many thanks to my second supervisor, Dr. M. Lubczynski, for welcoming me to his research group and for having the right comments, in the right time.

A special acknowledgement goes to Leonardo Reyes, who has been there to support me from the beginning to the end of the thesis period; who told me (unsuccessfully) how to take core samples of hard oak wood and many other things during fieldwork and who has taken a lot of time reading the drafts of this document thoroughly.

I would also like to thank Dr. Stanislaw Lewinski, from Warsaw University, Norman Kerle and Diana Chavarro from ITC, for their advice on object-oriented classification issues; Christiaan van der Tol and Joris Timmermans from the Water Resources Department of ITC for long time put on the examination of field data and DART files, respectively, and Ivar Ledezma, for his fundamental support on numerical methods. Finally, thanks to Zornitza Yovcheva for reviewing the first research proposal, to Pablo Argandonia for the drawings of the leaf chamber and to Jose Suarez, for helping always in these “small” technical issues.

To my colleagues, and now friends, in the Water Resources Department, for their chivalry during fieldwork and for very helpful comments, suggestions and academic exchange, those are reflected indirectly in this document.

This work is dedicated to my parents and to my brother, with lots of love.

Table of contents

1.	Introduction	10
1.1.	Research motivation.....	10
1.2.	Objectives	11
1.3.	Research Questions.....	11
1.4.	Hypothesis	11
1.5.	Review of methods for the estimation of evapotranspiration	12
2.	Materials and Methods	15
2.1.	Description of the study area	15
2.2.	Tree species classification and mapping.....	16
2.3.	Transpiration estimation by sap flow measurements	20
2.4.	Transpiration estimation by the Penman-Monteith model.....	22
2.5.	Upscaling transpiration using 2 different methods	26
2.5.1.	Upscaling transpiration to tree level.....	28
2.5.2.	Upscaling transpiration to stand level.....	30
2.5.3.	Upscaling transpiration to catchment level.....	33
3.	Results and Discussion.....	37
3.1.	Tree species classification and mapping.....	37
3.2.	Transpiration upscaling to tree level.....	42
3.3.	Transpiration upscaling to stand level	47
3.4.	Transpiration upscaling to catchment level	49
3.5.	Considerations on sources of error.....	51
4.	Conclusions	55
5.	References	57

List of figures

Figure 1 Reference map of the Sardón River basin. Modified after Lubczynski and Gurwin (2005).....	15
Figure 2. Mean spectral signatures taken from a Quickbird image of August 2009, for 10 pixels of <i>Q. Ilex</i> and <i>Q. Pyrenaica</i>	18
Figure 3 Methodological flowchart of the Multi-Criteria classification method.....	19
Figure 4 Location of the trees where sap flow and other measurements were taken.	22
Figure 5 Parabolic red line showing leaf area distribution over height.....	29
Figure 6 Trabadillo stand (on false colour satellite image) with corresponding canopy segmentation	31
Figure 7 Canopy sizes and their frequency distribution in the Sardón catchment. Quartiles are shown in blue vertical lines.	35
Figure 8 Spectral classification with object-oriented analysis	37
Figure 9 Multi-criteria classification results.....	38
Figure 10 Graphical explanation of map accuracy.....	41
Figure 11 Regression for sap flow-based transpiration at tree level against estimations derived from the “big leaf” approach ($T*CA/LAI$) and Gaussian integration method ($T*LAI_i$).....	44
Figure 12 Leaf temperatures for 12 samples of <i>Q. Ilex</i> and 15 samples of <i>Q. Pyrenaica</i>	47
Figure 13 Biometric Upscaling Functions.....	48
Figure 14 A canopy of <i>Q. Pyrenaica</i> modified by pruning and by cattle. ..	52

List of tables

Table 1 Climate indicators of the Sardón River Basin. Modified after Lubczynski and Gurwin (2005).....	15
Table 2 Variables needed to estimate transpiration by the Penman-Monteith model and the proposed way to estimate them. Source (Dingman 2002)	23
Table 3. Common approaches and scalars used in tree transpiration upscaling.....	27
Table 4 Error matrices for accuracy assessment. Based on (Pilesjo 2009) ..	39
Table 5 z test to define confidence intervals	40
Table 6 Kappa statistics for the two classification methods.....	40
Table 7 McNemar's test for dependent samples	41
Table 8 Transpiration calculation for a single tree from sap flow measurements	42
Table 9 Results of transpiration upscaling at stand level using sap flow measurements	49
Table 10 Calculation of total tree transpiration in the Sardón catchment using the quartiles (Q) of canopy area distribution.	50

1. Introduction

Water Limited Environments (WLE) are sub-humid to arid areas, where the annual ratio of precipitation to potential evapotranspiration lies between 0.03 and 0.75 (Abrahams and Parsons, 1994). Given these dry conditions, the availability of water is central for the functioning of ecosystems. The use of water by plants, also called transpiration, plays a major role in the water balance of WLE and is thus of a major importance in water assessments for conservation and regional planning.

Transpiration is a complex process that depends on variables that can be difficult to estimate for different scales and under time/equipment/budget constraints. This study revises common approaches to estimate transpiration at different spatial scales, aiming to obtain a better understanding of the data requirements and uncertainties associated with each, and their suitability for different applications. Knowledge about the magnitude of water consumption by vegetation will not only contribute to the improvement of water balance estimations in WLE, but will also create awareness of the ecosystem services of vegetation, unveiling opportunities for development and conservation in otherwise disregarded arid areas.

1.1. Research motivation

The elements of the water balance that are particularly of interest in the context of Water Limited Environments are recharge and evapotranspiration, which vary not only temporally, but also spatially. Considering that these variables are affected by soil and plants characteristics, the distributed water modelling in WLE requires detailed information in order to represent the landscape, ecosystem functions and water availability accurately.

The techniques for the estimation of evapotranspiration (hence, water and soil evaporation and plant transpiration) are well known, but a challenge remains regarding adequate parameters to represent it at different scales, given the plant- and site-specific nature of the estimations. Methods based on remote sensing for example, generally overestimate ET and there are difficulties in separating soil evaporation from plant transpiration. As a corollary, indirect approaches to estimate transpiration (and thus evapotranspiration) may not apply at all spatial scales. There is the need to find reliable criteria to represent transpiration rates based on field measurements at local and regional scales.

1.2 Objectives

General objective:

Compare the estimations of tree transpiration in a Water Limited Environment obtained by two different methods and investigate the best options to upscale the field measurements to the stand and basin scale.

Specific objectives:

- a) Classify tree species in the Sardón catchment using an object-oriented approach on a high resolution satellite image.
- b) Assess individual tree transpiration by sap flow measurements and upscale tree transpiration using relations between crown area and sapwood area.
- c) Assess individual tree transpiration by the Penman-Monteith model and upscale tree transpiration using leaf area, crown area and the fraction of vegetation cover
- d) Compare the up scaled transpiration estimates obtained by sap flow measurements and the Penman-Monteith model

1.3 Research Questions

- a) Can the custom classification parameters of an object-oriented approach yield high classification accuracy?
- b) What are the sources of error related to the transpiration scalars?
- c) What is the agreement between estimated and observed variables needed to upscale tree transpiration (e.g. stomata conductance, Leaf Area Index)?

1.4 Hypothesis

- a) A higher proportion of trees are correctly classified by an object-oriented method than by a pixel-based method.

- b) The linear regression of transpiration estimations made with sap flow measurements and with the Penman-Monteith model at tree level has a slope close to 1 and an offset close to 0.

1.5 Review of methods for the estimation of evapotranspiration

Diverse approaches have been adopted through the years for the estimation of evapotranspiration (ET), considering it as the combined process of soil and water evaporation (E) and transpiration of vegetation (T). The most important of them have been reviewed by Dingman (2002). Traditionally, methods based on field measurements have been applied for small areas and for crop monitoring (Walter et al., 2005) while methods based on remotely sensed data are used at a regional scale (NASA, 2009) and (EARS, 2009).

Among the methods relying on field measurements, the FAO56 method, based on the Penman-Monteith equation (Allen et al., 1998), and the eddy covariance method (Koestner et al., 1992) are based on a mass transfer approach (Dingman, 2002). Other field-based methods use a pan (Snyder et al., 2005), lysimeters (Abteu and Obeysekera, 1994), scintillometers (Bastiaanssen et al., 2005) or sap flow measurements (Cienciala et al., 2000).

From all these methods, the FAO56 is the most widely used, especially for agronomic applications. It considers a reference ET factor, a crop ET factor and an adjusted crop ET factor. The method is based on the assumption that the reference crop is grass, the crop ET is a value under optimal water availability conditions and the adjusted ET represents the crop under stress conditions. It makes use of an experimentally determined crop coefficient, based also on the reference crop. Interestingly, the method is being used extensively in agronomy, though not so much in forestry.

In the last decades, the development of remote sensing techniques has contributed significantly to the spatial and temporal study of ET (Immerzeel et al., 2006). The methods based on remote sensing observations have been classified by Courault, Seguin et al. (2005) into Empirical Direct Methods, Residual Methods of Energy Budget, Deterministic Methods and Vegetation Index Methods.

Remote sensing methods generate surface parameters on a pixel scale and are therefore more suitable for spatial modelling of ET. The Empirical Methods are

based on simple relationships, for example between thermal infra-red reflectance and meteorological data. The main assumptions are that the daily ET is related to the difference of atmospheric temperature and surface temperature; the ratio of sensible heat flux and net radiation is constant along the day and that the daily soil heat flux is negligible (Courault et al., 2005).

Models that calculate ET as a residual of an energy or water balance, like SEBAL (Bastiaanssen et al., 2005) and SEBS (Su, 2002), generate a series of atmospheric variables from remote sensing data and assume semi empirical relations to estimate emissivity and surface roughness. To calculate the sensible heat flux, an area is divided into wet and dry land (Courault et al., 2005).

Deterministic methods are based on the soil-vegetation-atmosphere relations use models for its characterization. . These methods are diverse in complexity; the simple ones model ET for an area as the ET of a single big leaf and the complex ones are multi-layer models where energy balances are computed for each canopy layer, like DART (Gastellu-Etchegorry et al., 1996), SCOPE (Van der Tol et al., 2009) and ENVI-met (Samaali et al., 2007). Transpiration of vegetated areas and evaporation from soil is computed separately, with different values of surface resistance.

Finally, the Vegetation Index methods calculate a reference ET from field measurements and use remote sensing to estimate reduction factors, such as the adjusted crop coefficient required by the FAO56 method (Courault et al., 2005).

The methods described above allow the easy determination of the soil, water and plant transpiration components of ET. Some of them have been adapted for calculations at different time intervals (Gieske and Meijninger, 2005; Moran et al., 2009), or to obtain actual ET (Droogers, 2000). Nevertheless, some parameters are still difficult to estimate (e.g. stomata resistance) and thus models are not always able to represent water-stress conditions accurately, because of generalizations or assumptions on temporal and/or spatial variability of the mentioned parameters. On the other hand, site-specific models, with accurate specification of the concerned parameters, are not suitable for regional studies.

In general, the adoption of methods based on remotely sensed data for regional studies has become a common practice given the difficulties in upscaling field measurements accurately. But scientific literature is still silent about the performance of these methods at different spatial scales and the related errors. In this respect, the opinion of Ford, Hubbard et al. (2007) is remarkable: “Our ability to accurately scale from the probe to the tree to the watershed has not yet been demonstrated, nor do we know the relative impact of the main sources of variability

on our scaled estimates. Accounting for the variability in the radial distribution of sap flux within the sapwood, the variability of transpiration among trees and between plots within the catchment, and the variability in stand density, sapwood area, and leaf area are critical for making landscape inferences about transpiration”.

2. Materials and Methods

2.1. Description of the study area

The Sardón River catchment is located in the western part of the Iberian Peninsula, about 50 Km from the city of Salamanca (Figure 1), between 6°07' and 6°13' W and 41°01' and 41°08' N (Habtemannian, 2000). It is a catchment formed on massive and fractured granite, with a thin superficial layer of weathered material, where the geological structures control the hydrological and morphological processes according to two well differentiated seasons (Lubczynski and Gurwin, 2005). The Sardón River lies on a fault zone, which remains almost dry from June to October, and where big discharges can be observed during and after heavy rain showers in the rainy seasons.

Table 1 Climate indicators of the Sardón River Basin. Modified after Lubczynski and Gurwin (2005)

Warmest, driest months	July, August	Coldest months	January, February
		Wettest months	November, December
Temperature	~22 °C	Temperature	~5 °C
Potential ET	~5 mm/d	Potential ET	~0.5 mm/d
Rainfall	< 20 mm/month	Rainfall	> 100 mm/month

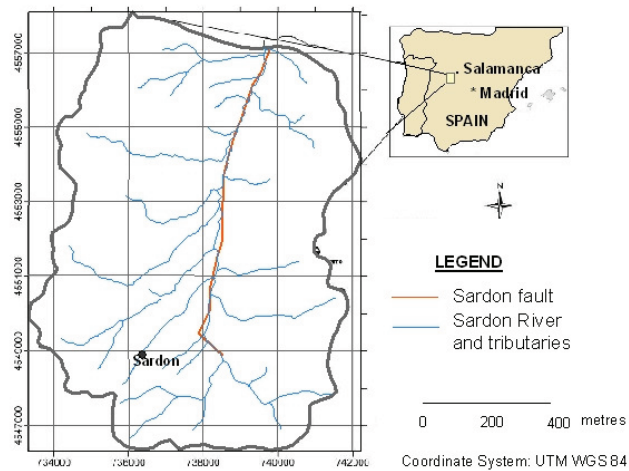


Figure 1 Reference map of the Sardón River basin. Modified after Lubczynski and Gurwin (2005)

Vegetation in the area consists mainly of oak trees, grasses and shrubs (*Cytisus scoparius*). From these, the phreatophyte *Quercus ilex* plays an important hydrogeological role, as 70% of its transpiration is of groundwater origin (David et al., 2007)

The 80 Km²-catchment is sparsely populated, with low impact of cattle breeding activities. It has been selected for this study not only because it is a representative Water Limited Environment, but also because of the availability of meteorological data, acquired by two Automatic Data Acquisition Systems (ADAS) since 1987, sap flow measurements since 2001 and eddy covariance measurements.

Moreover, a decade of academic output in the area (Rwarinda, 1996; Habtemannian, 2000; Nakamba, 2002; Ontiveros, 2009) constitute a suitable knowledge base of the basic environmental patterns of the area and allow an in-depth study of tree transpiration.

2.2. Tree species classification and mapping

In order to know the spatial distribution of tree transpiration (T), it is first necessary to determine the spatial distribution of the tree species in the study area. Kimani (2004) discusses several experiences of forest classification for sap flow upscaling and concludes that object-oriented classification is more suitable than pixel-based classification. Analyzing individual objects of the satellite image (trees in this case) has also the advantage of considering texture and contextual information for the classification, and not only spectral information. Moreover, “ecologically speaking, it is more appropriate to analyze objects as opposed to pixels because landscapes consist of patches and because objects in a landscape are scale-dependent” (Kimani, 2004; Laliberte et al., 2004). Yan, Mas et al.(2006) report 36.7% higher accuracy of object-oriented over pixel-based forest classifications.

The experiences of Kimani (2004), who classified dry savannah vegetation in Botswana, and Ontiveros (2009), who performed a tree classification of the Sardón catchment using aerial photographs, reveal that the classification requires segmentation in different spectral bands and a satellite image with high spatial resolution. In this study the visible and infra-red channels of a Quickbird image (with spatial resolution of 2.4 m) were used in the Definiens Developer 7 software (Definiens, 2007) for the tree classification of the Sardón catchment.

In order to perform transpiration upscaling, the canopy areas of individual trees and their correspondent species have to be known. Therefore, a stepwise procedure was executed: first, image segmentation and second, classification.

The segmentation of the satellite image was carried out so that each tree of the catchment represents an object. This step is fundamental to assure accuracy and representativeness of the final output. Individual trees were identified from the rest of the image using the Quadtree segmentation algorithm and the maximal difference in their pixel values (Max. value – Min. Value/Brightness).

The second step in the classification is the differentiation of the two tree species living in the area. This represented a more complex procedure because on the image taken on August 2009, the spectral signatures of the species in the visible spectrum overlap (Figure 3). Also, the morphology features seen in the image are similar for the two species. An additional problem was the separation of tree canopies into shaded, totally sunlit and partially sunlit areas. The shade made difficult the accurate determination of the western boundary of the canopies, and the sunlit areas have similar reflectance in both species. To overcome these difficulties, three procedures for classification were proposed: i) to use the spectral information from a supervised classification and then fine-tune the results using an object-oriented approach; ii) to use context information, field observations and “expert knowledge”¹ besides spectral information, applying a Weighted Linear Combination in the context of a Multi-Criteria Evaluation (Eastman, 2006); iii) to apply fuzzy set memberships to the criteria mentioned in ii). This last option could not be tested due to time limitations.

¹ This term includes non-published, specific knowledge about the study area and/or the studied species, which has been gained through the years by different professionals working in topics related to this study. It also refers to the decision criteria used for classification.

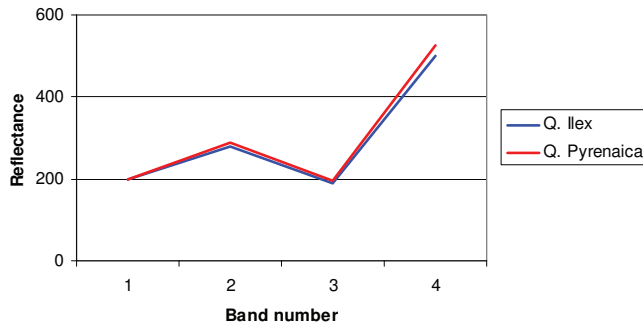


Figure 2. Mean spectral signatures taken from a Quickbird image of August 2009, for 10 pixels of *Q. Ilex* and *Q. Pyrenaica*

The first procedure was developed in collaboration with PhD candidate Leonardo Reyes from ITC, and processed using Erdas Imagine 9.3. First, the Quickbird image was classified into 60 classes using a pixel-based, unsupervised classification of the red and near infra-red bands, as they have the higher reflectance for vegetation (Janssen, 2001). Secondly, this classification was refined by a supervised routine of selecting classes with the same features and merging them to finally obtain 40 classes, 15 of them corresponding to tree classes. At this point, the classified image shows individual trees with a mixture of pixels classified both as *Quercus Ilex* and *Quercus Pyrenaica*. Finally, to determine the species of each tree, it was decided to assign a class to a tree if the majority of the pixels were classified previously to that class. This was done by calculating the relative area of each class inside each tree object and then re-classifying the image.

In the second procedure, GIS (ArcGIS 9.3) was used as the platform in managing, combining and displaying the criterion data and also as a tool for producing new data, especially by using spatial analysis functions. The flowchart in Figure 5 shows the methodology used by this classification method. Continuous criteria were standardized to a common numeric range and then combined by weighted averaging. The criteria used for the tree classification were the following:

- Rocky areas have mostly only *Quercus Ilex* trees
- As *Quercus Ilex* is a phreatophyte species, it is located in areas where the water table is deep. In areas with shallow water table (e.g. close to the rivers), more individuals of *Q. Pyrenaica* were observed.

- *Q. Pyrenaica* has higher reflectance in the Near Infra-Red band than *Q. Ilex* at the time of image acquisition (August 20th, 2009)

In order to identify rocky areas, a physiographic classification of the image was obtained with a multi-resolution segmentation algorithm and a coarse scale parameter. Only spectral information was used at this stage due to the relative easy differentiation of physiographic units in the spectral domain.

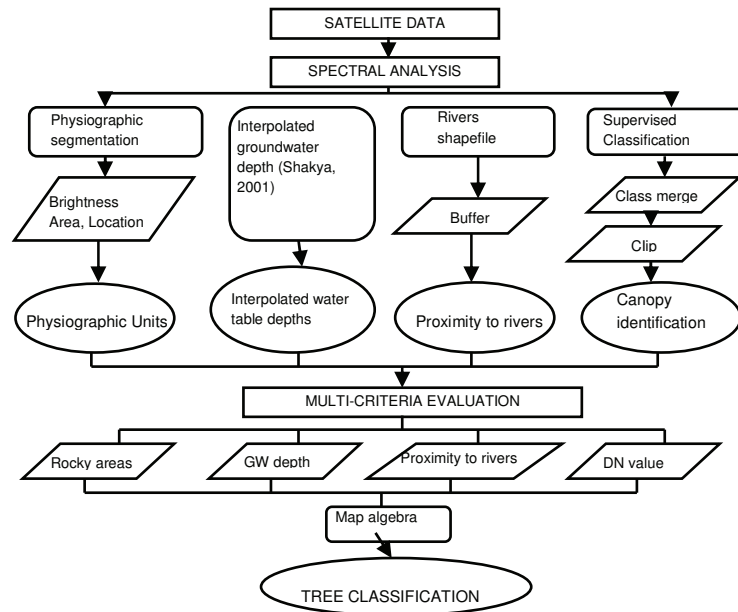


Figure 3 Methodological flowchart of the Multi-Criteria classification method

Finally, each of the classifications obtained with the above-mentioned procedures was subject to an accuracy assessment test, carried out with an error matrix (Table 2) (Congalton, 1991; Pilesjo, 2009) and species information for 310 trees collected in the field by the author and other MSc students using GPS positioning. Kappa values were then computed to assess the influence of chance in the classification.

To test the significance of the difference between the Kappa values, z-tests are usually applied (Im and Jensen, 2005; Bowes et al., 2007). De Leeuw, Schmidt et al.(2002) demonstrated that if the same sample points are used to evaluate two maps, there is a dependency between the error matrices and thus a smaller variance of the difference in sample proportions as compared to independent sample point sets. The

authors proposed to use the McNemar’s test for dependent proportions (McNemar, 1947), which uses a chi square statistic, calculated as follows:

$$x^2 = (f_{12} - f_{21})^2 / (f_{12} + f_{21}) \quad [\text{Eq. 1}]$$

Where f is the number of classified points according to the error matrix.

Table 2 Example of an error matrix

Classifier 1	Classifier 2		Total
	Wrong	Correct	
Wrong	f_{11}	f_{12}	
Correct	f_{21}	F_{22}	
Total			

The results of the accuracy assessment are explained in Chapter 3 and reported in Tables 5, 6 and 7.

2.3. Transpiration estimation by sap flow measurements

The movement of water through 3 trees of each species (Figure 4) was monitored either by the Granier method (Granier, 1985), or by the Heat Field Deformation (HFD) method (Nadezhdina et al., 1998) during August and September 2009, at 30 second and 10 minute intervals, respectively. The data is part of the monitoring network established for an ongoing PhD research (Reyes, unpublished).

Although both of the above mentioned methods are based on measurements of thermal conductivity of sap (also known as sap flux density) in one or more parts of the stem (“point” methods, see Figure 4), they also have important differences; the first one being the knowledge base of each method. Andre Granier developed his method in the 1980s and the widespread use of this technique has even lead to commercial and “home made” variants of the original sensors (Lu et al., 2004). The Heat Field Deformation (HFD) method on the other hand, is the newest technique developed for sap flow monitoring, with physical analysis still being carried on and further improvements to be expected (Čermák et al., 2004).

Another difference is the longitude of the needle-like thermo-couple that is inserted into the stem. Granier sensors have 2 cm length, whereas HFD sensors measure 7.5 cm. That means that only the first 2 cm of conductive sapwood can be measured by the Granier method. In the case of the Sardón catchment, better estimations of sap flux density using Granier sensors can be obtained for *Q. Pyrenaica*, because the outer part of the sapwood conducts most of the flow (CITATION), whereas sap flow in *Q. Ilex* is concentrated in the deeper parts of the sapwood (Figure...). These considerations are important for this study, because in order to use the two sap flow methods simultaneously, HFD data from the first 2 cm of sapwood could be used.



Figure 4 Granier and HFD probes inserted into oak stems. The sensors were later protected from the sun and animals with stereopor and wire nets (picture of Granier sensors from Mapanda (2003)).

Data around the 15th and 17th of September were used in this study to enable comparison of transpiration estimations with the Penman-Monteith transpiration calculations made for the same days. In order to calculate the tree transpiration rate, the xylem area for each tree was first calculated by taking wood samples with a Pressler borer in the field. Xylem length was measured after dying the samples with Methyl-Orange. The dying allowed the visual recognition of core wood from sapwood and bark. The xylem and hardwood were measured with a small calliper and the bark length was assumed constant at 1 cm for *Q. Ilex* and 1.5 cm for *Q. Pyrenaica*. Once the length of the bark, the xylem and the hardwood were known, the total xylem/sapwood area of the trunk could be calculated with Equation 2 (see below). The transpiration rate for each measured tree was finally estimated multiplying the sap flux density by the sapwood area.

$$A_x = \left[\pi * \left(\frac{DBH - (2 * bark)}{2} \right)^2 \right] - \left[\pi * \left(\frac{DBH - (2 * bark) - (2 * xylem)}{2} \right)^2 \right]$$

[Eq. 2]

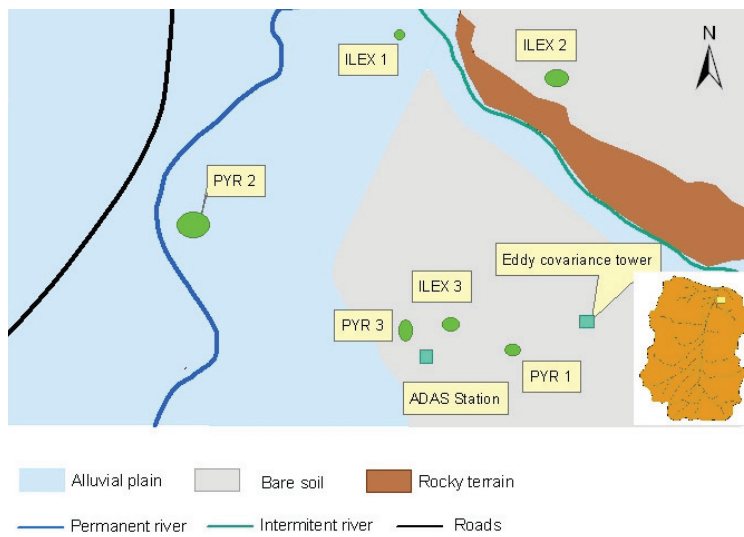


Figure 5
Location of the trees where sap flow and other measurements were taken.

2.4. Transpiration estimation by the Penman-Monteith model

Transpiration is the process whereby water is evaporated from the leaf surface of trees or any other type of vegetation, and thus the terms transpiration and leaf evaporation are used often with the same meaning. “The vaporization occurs within the leaf, namely in the intercellular spaces, and the vapour exchange with the atmosphere is controlled by the stomata aperture” (Allen et al., 1998).

Howel and Evett (n.d.), Dingman (2002) and NASA (2009) show the sound and solid theoretical development of the Penman-Monteith method – which has a thermodynamic and an aerodynamic component – for the calculation of surface evaporation in vegetation. The corresponding FAO56 methodology (Allen et al., 1998) has been internationally accepted as a standard method.

The model is based on the following equation (Dingman, 2002) and the variables are described in Table 3:

$$E_{leaf} = \frac{[\Delta * (K + L) + \rho_a * c_a * g_{at} * e_a * (1 - W_a)]}{\left[\rho_w * \lambda_v * \left(\Delta + \gamma * \left(1 + \left(\frac{g_{at}}{g_{can}} \right) \right) \right) \right]} \quad [\text{Eq. 3}]$$

Where

Table 3 Variables needed to estimate transpiration by the Penman-Monteith model and the proposed way to estimate them. Source (Dingman, 2002)

Variable	Origin/Value	Units
E_{leaf} = evaporation from a leaf surface		Kg/ m ² /h
Δ = temperature of the air – temperature of the canopy	Derived from meteorological and field data	Dimensionless (temperatures measured in °C)
K= atmospheric constant	Derived from ρ_a	Pa ⁻¹
L = long wave energy exchange	Derived from $\rho_w, \lambda_v, K, e_a$	W/m ²
ρ_a = density of air	Derived from meteorological data	Kg/m ³
c_a = heat capacity of air	1.0*10 ⁻³	MJ/kg/K
e_a = saturation vapour pressure at the air temperature	Derived from meteorological data	Pa
W_a = relative humidity	Derived from meteorological and field data	%
ρ_w = mass density of water	1000	kg/m ³
λ_v = latent heat of vaporization	2.257	J/Kg
γ = psychrometric constant	0.06	Pa/C
g = surface conductance g_{can} = canopy conductance g_{at} = atmospheric conductance	Derived from field data	Measured in mmol/m ² /s; expressed in m/s for

		calculation
--	--	-------------

The atmospheric component of Equation 3, given by the atmospheric conductance (g_{at}) and the atmospheric constant (K), represent “the efficiency of the turbulent eddies in the lower atmosphere in transporting water vapour from the surface of the leaf to the ambient air” (Dingman, 2002). The formulas are described below.

$$K = \frac{0.622 * \rho_a}{P * \rho_w} \quad g_{at} = \frac{v_a}{6.25 * \left[\ln \left(\frac{z_m - z_d}{z_0} \right) \right]^2} \quad [\text{Eq. 4, 5}]$$

Where

K= atmospheric constant

ρ_a = density of air

P = atmospheric pressure

ρ_w = mass density of water

g_{at} = atmospheric conductance (m/s)

v_a = wind speed (m/s)

z_m = height of wind speed measurement (10 m)

z_d = zero-plane displacement height = $0.7 * z_{veg}$

z_0 = roughness height = $0.1 * z_{veg}$

z_{veg} = vegetation height (m)

Vegetation height was taken as the average value of the height of sampled trees in the field. The values are 6.65 m for *Q. Ilex* and 8.56 m for *Q. Pyrenaica*.

The thermodynamic component of Equation 3 is represented by the latent heat of vaporization and the long wave energy exchange, besides the air and leaf temperatures. The first is the energy required to vaporize 1 Kg of water; this is 2.257 Joules. The second is a residual from the energy balance of the study area.

Infante, Rambal et al.(1997) demonstrated a high degree of coupling between the atmosphere and the canopy in evergreen oaks of the Iberian Peninsula (mean decoupling coefficient of 0.2 for *Q. Ilex*), both at the leaf and tree level. This allows a simplification of the Penman-Monteith model at the mentioned scales, so that Equation 3 reduces to (David et al., 2007)

$$E = g * D * \left(\frac{\rho_a * c_a}{\lambda * \gamma} \right) \quad [\text{Eq. 6}]$$

Where D is vapour pressure deficit of the air (in Pa) and all other terms are as described in Table 3.

Wind speed, air temperature, air pressure and relative humidity data (15th to 17th of September, 2009) from a meteorological/eddy covariance tower installed in the northern part of the Sardón catchment were used. These data were acquired during the measurement dates of leaf conductance in the field, carried out with the CI-340 Photosynthesis Instrument (CID, 2003). This instrument uses a chamber to isolate a leaf for measurement (Figure . It measures the gas exchange (CO₂ and H₂O) of the leaf with the chamber environment, to calculate leaf conductance, photosynthesis rate, leaf temperature, PAR and evaporation at the leaf surface. The equation used by the instrument for leaf stomata conductance is the following

$$g_{leaf} = \frac{W}{\frac{e_{leaf} - e_o}{e_o - e_i} * \frac{P - e_o}{P} - R_b * W} * 1000 \quad [\text{Eq.7}]$$

Where

g_{leaf} = leaf stomata conductance (mmol/m²/s)

W = mass flow rate per leaf area (mmol/m²/s)

e_{leaf} = saturated water vapour at the leaf temperature (bar)

e_o = outlet water vapour (bar)

e_i = inlet water vapour (bar)

P = atmospheric pressure (bar)

R_b = leaf boundary layer resistance: 0.3 m² s/mol is used

In order to use the measured leaf conductance in Equations 3 and 4, which require canopy conductance as input, it is necessary to multiply it by the leaf area

and a factor to account for the fact that some leafs are partially or totally shaded by other leafs within a canopy and thus transpire less. Values of the shelter factor vary between 0.5 and 1, and decrease with increasing LAI (Carlson, 1991 in Dingman, 2002)

$$g_{can} = g_{leaf} * LAI * f_s \quad [Eq. 8]$$

Where

g_{can} = canopy conductance (m/s)

g_{leaf} = leaf conductance (m/s)

LAI = Leaf Area Index (dimensionless)

f_s = shelter factor: 0.6 for Q. Ilex and 0.4 for Q. Pyrenaica

Due to the fact that leaf conductance is calculated from gas exchange, proper calibration of the instrument is of utmost importance; daily calibration was carried out with special devices that are part of the instrument set. Nevertheless, an overheating of the chamber was observed after some hours of measurement in the field, possibly because the instrument was exposed directly to the sun during measurements. To correct leaf temperatures values, a set of thermo probes were attached to the leaves and the corresponding measured voltage was transformed into temperature values with aid of the HOBO 2.6.0 software.

2.5. Upscaling transpiration using 2 different methods

Once transpiration had been estimated by each method, it was possible to upscale the measurements at different levels: from leaf to canopy, from canopy to stand, and from stand to basin. This was done in order to establish the agreement between methods and between variables needed for upscaling (research question c). Table 4 shows different upscaling parameters for water uptake and leaf evaporation.

Table 4. Common approaches and scalars used in tree transpiration upscaling.

Transpiration estimated by sap flow measurements		
<i>Stem – Tree</i>	<i>Tree – Stand</i>	<i>Stand - Catchment</i>
Diameter at Breast Height	Effective width of trees (Crosbie et al., 2007)	Fraction of Vegetation Cover [proposed by the author]
Sapwood area (Chavarro-Rincon, 2009)	Biometric Upscaling Function (Lubczynski, 2009)	Total crown cover (Shakya, 2001)
	Scaling curves (Čermák et al., 2004)	
Transpiration estimated by the Penman-Monteith model		
<i>Leaf to Canopy</i>	<i>Canopy to Stand</i>	<i>Stand to Catchment</i>
Assume the canopy is a single “big leaf” and use LAI (Dingman, 2002)	Leaf Area Index (LAI)	Fraction of Veg. Cover [proposed by the author]
Canopy leaf distribution represented by a logarithmic function (Goudriaan, 1986)	Effective width of trees (Crosbie et al., 2007)	Scaling curves (Čermák et al., 2004)
Radiative Transfer Models (Gastellu-Etchegorry et al., 1996; Samaali et al., 2007; Van der Tol et al., 2009)		

The multi-scale estimation of tree transpiration and evapotranspiration in general, is a complex task, involving many variables, obtained generally from different sources. Given this complexity, it is necessary to clearly define the scope of this study and make some assumptions in order to avoid deviations from the objectives. The following are the statements and assumptions that have been considered:

- This study focuses only on the *spatial* variability of the drivers of tree transpiration. For best results, data collected during mid-day hours has been used. This is a time in the day where the temporal variability of transpiration is lower (Van der Tol et al., 2007)

- There is no sub-pixel variability. A Quickbird satellite image of 2.4 m resolution has aided in many stages of the upscaling process. This pixel size is smaller than most of the canopies of the trees in the Sardón catchment.

- The sun angle and environmental conditions at the time of image acquisition (August 20th, 2009) can be considered equal to those at the time of temperature measurement (15-17th September, 2009, between 11:30 and 14:30).

- The effects of micro-topography on aerodynamics are considered negligible in the Sardón catchment, thus, this variable was not considered.

- The sapwood area in a tree stem is assumed to be constant. This assumption was made for practical reasons, despite general acknowledgement of a significant variation of sapwood area for a number of tree species. This study will investigate other sources of error; for example, the influence of canopy temperature. The reader is referred to the work of Poyatos, Cermak et al.(2007) for a study of sapwood variability in transpiration estimations.

- No stem storage of water was considered, thus sap flow represents transpiration.

- The effects of aerodynamics are not significant at the leaf, canopy and stand levels. Oak trees from the Mediterranean region are highly coupled from the atmosphere (Infante et al., 1997)

- Meteorological measurements taken at the northern part of the study area are representative of the whole Sardón catchment.

2.5.1. Upscaling transpiration to tree level

Sap flow represents the transpiration at the tree level and thus further calculations are not needed. In contrast, the Penman-Monteith method relied on measurements of gas exchange at the leaf level, so a first upscaling procedure is necessary to make both estimations comparable.

To establish transpiration from leaf measurements, the description of the geometry of the canopy is of crucial importance. The approaches go from the simplistic method of assuming the transpiration of a canopy as that from a single big leaf (Dingman, 2002) to a detailed model of a canopy, consisting of layers with different Leaf Area Index (LAI), leaf angle and inclination (Verhoeff, 1997; Van der Tol et al., 2009). The intermediate approach introduced by Goudriaan (1986) uses a parabolic function to describe the leaf distribution of a canopy. The two first methods are comparable and have therefore been tested.

The “Big Leaf” upscaling approach was adopted by simply multiplying the leaf transpiration values obtained in the field by the corresponding LAI of the species.

The Goudriaan method takes into account the different distribution of leaves in a canopy, in terms of the Leaf Area Index (LAI). The vertical profile of a canopy is

the result of a differentiated leaf distribution, depending on the tree species and the structure of the canopy, i.e. presence of holes. (Figure 6)

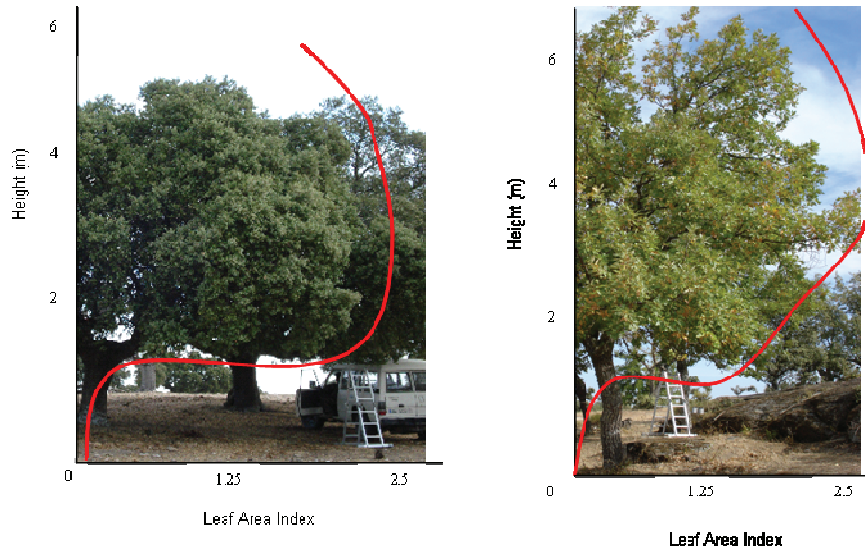


Figure 6 Parabolic red line showing leaf area distribution over height

LAI was measured at 4 discrete heights of the canopy using the LAI2000 instrument. Then, values were integrated using a 4-point Gaussian integration (Goudriaan, 1986) to calculate the total leaf area of the canopy. “This method specifies discrete points at which the value of the function to be integrated has to be calculated”; these are the heights at which LAI was measured. “It also defines the weighting factors that have to be applied to these values to obtain an accurate approximation compared to the analytical solution” (Kropff and van Laar, 1993).

The transpiration rate measured at the leaf level was finally multiplied by the total leaf area in order to obtain the transpiration value for a single tree of each species.

2.5.2. Upscaling transpiration to stand level

2.5.2.1 Upscaling based on sap flow measurements

Crosbie et al. (2007) propose a method that accounts for the “hydrological” area occupied by a tree. This includes an area underground (occupied by roots), an area at the ground surface (sapwood area in each stem) and an area above ground (occupied by the tree crown), that can be measured in the field, observed in aerial photographs, and/or adopted from botanical literature. As the fieldwork supporting this study did not include root assessment, and adopting values from literature may introduce errors, a linear method based only on canopy areas was adopted.

Transpiration can be calculated from the relationship of sapwood area and canopy area of a tree. This last relation is given by an empirical Biometric Upscaling Function (Chavarro-Rincon, 2009; Lubczynski, 2009), which has been established for each species by measuring canopies and xylem for 23 *Q. Ilex* trees and 20 *Q. Pyrenaica* trees in different areas of the Sardón catchment. Data for these trees has been collected and processed in collaboration with other MSc students (Agbakpe, 2010; Rwasoka, 2010).

The segmentation file created for the species classification (Chapter 2.2) was used to calculate the canopy area. Some polygons of this file did not delineate the canopies perfectly, so it was decided to calculate the canopy projected area with the following equation that approximates the shape of a canopy to that of an ellipse:

$$A_c = \pi * \frac{a}{2} * \frac{b}{2} \quad [\text{Eq. 9}]$$

Where a = mayor axis of the ellipse

b = minor axis of the ellipse

The properties “Length” and “Width” were displayed for each object in the Definiens software and then exported as a shape file, where the area could be calculated using the Field Calculator function. The length and width of each tree crown correspond to the major and minor axes of an ellipse.

Then, a stand of 1 ha was selected in the area where sap flow of the Pyr1, Pyr3 and Ilex3 trees was measured (Table 2). It lies in the northern part of the Sardón catchment, in the Trabadillo area, close to the mouth of the Sardón River (Figure 8).

The following formula was used for upscaling:

$$T_{st} = \sum T_s * \frac{CAs}{CA_t} \quad [\text{Eq. 10}]$$

Where T_{st} is stand transpiration; T_s is sample transpiration; CAs is canopy area of the sampled trees and CA_t is total canopy area of the stand. This formula can also be used with any other biometric parameter that can be related to tree transpiration, e.g. diameter at breast height or sapwood area. (Čermák et al., 2004)

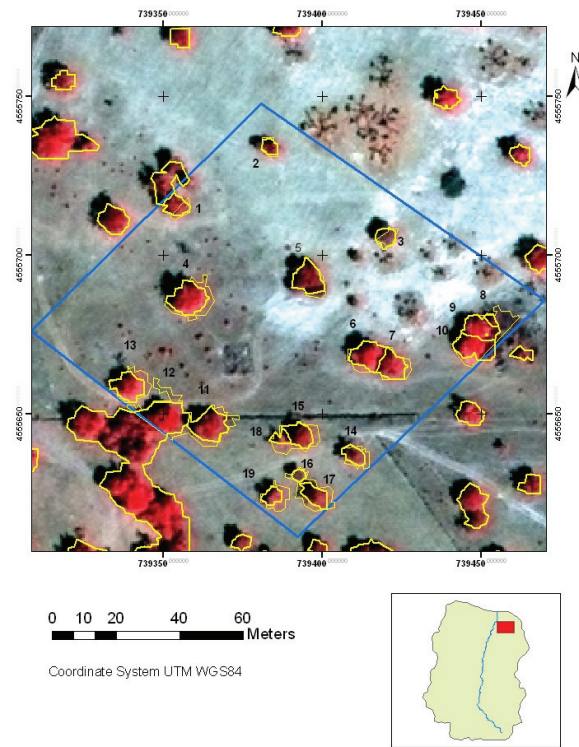


Figure 7 Trabadillo stand (on false colour satellite image) with corresponding canopy segmentation

2.5.2.2

Upscaling based on the Penman-Monteith model

Transpiration calculations have been done for the Trabadillo stand, taking them as estimated values to be compared with observed sap flow-based transpiration estimates. The rationale for upscaling is explained as follows.

The most important variables that influence transpiration spatially and temporally are radiation, vapour pressure deficit and stomata conductance. They interact strongly between each other, posing opportunities and challenges for upscaling: on one hand, as one variable changes, the others change as well, which enables the researcher to estimate transpiration as a function of only one of these variables. On the other hand, the variation of the mentioned transpiration drivers is of different magnitude, and also variable among plant species and water availability conditions.

For this part of the study, transpiration has been modelled as a function of radiation, and specifically of temperature. The portions of the canopy that receive more radiation have higher surface temperatures, and the vapour pressure deficit between canopy and atmosphere is also higher. Temperatures for the air were obtained from 5 minute-readings of a meteorological instrument mounted on a tower at about 300 m from the stand. Temperatures for 16 sunlit and 16 shaded leaves of each species were measured in the field and the median values were adopted for the corresponding canopy portion. Next, the total canopy temperature for each tree was calculated as the weighted average of sunlit and shaded leaf temperatures, according to their extent in the satellite image. A Quickbird image acquired on August 20th, 2009, at 11:32 am was used for this purpose.

Vapour pressure deficit is a function of temperature, and thus it has been estimated from the temperature data.

Stomata are the pores of the leaf, which open and close depending on the radiation and pressure levels between the leaf surface and the surrounding air. The measure of their openness is called stomata conductance, in analogy to an electric circuit, and is expressed in units of mass per units of area per units of time, or in velocity units. Its variation with meteorological variables is also influenced by environmental factors such as drought. The measurements of gas exchange on which the stomata conductance values used in this study are based on (Chapter 2.4) were taken at the end of summer, a period known for water scarcity in the Sardón catchment (Table 1).

The formula used with this temperature-adjusted “Big Leaf” upscaling approach is

$$T_{st} = \frac{\sum_i^j [(T_s * w_s) + (T_{sh} * w_{sh})]}{A} \quad [\text{Eq. 11}]$$

Where

i and j are the two tree species

T_s is the stand transpiration rate ($\text{kg/m}^2/\text{s}$)

T_{sh} is the transpiration rate of the sunlit part of the canopy ($\text{kg/m}^2/\text{s}$)

w_s is the area of the sunlit part of the canopy, expressed as a percentage of the total canopy area

T_{sh} is the transpiration rate of the shaded part of the canopy ($\text{kg/m}^2/\text{s}$)

w_{sh} is the area of the shaded part of the canopy, expressed as a percentage of the total canopy area

A is the area of the stand m^2

The supervised classification used for the tree species classification was used to measure the extent of sunlit and shaded parts of the canopies. As can be seen in Figure 4, a single tree had been preliminarily divided into tree classes: sunlit parts of the canopy as *Q. Pyrenaica*, shaded parts of the canopy as *Q. Ilex*, and shadows as shadows.

2.5.3. Upscaling transpiration to catchment level

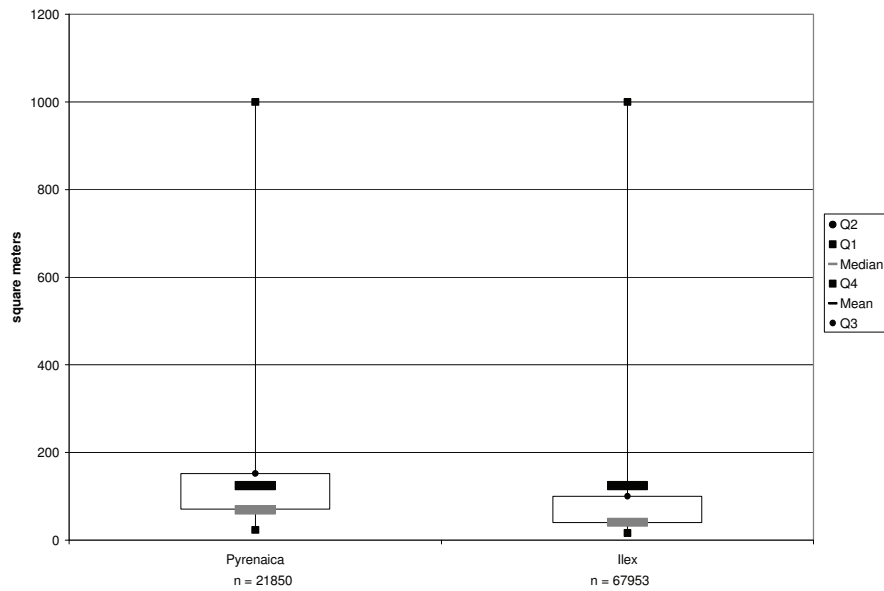
2.5.3.1 Upscaling based on sap flow measurements

According to Lubczynski (2009), LAI is suitable for upscaling “but its application in WLE is questionable because leaf turnover is slow while transpiration varies rapidly in response to changing environmental conditions (Wullschleger et al. 1998)”. A relationship based again on canopy area seems to be thus appropriate and easy to obtain using the species classification. Shakya (2001) proposes to estimate catchment transpiration with the following equation:

$$T = \frac{\sum CC_{i,j} * SF_{i,j}}{A} \quad [\text{Eq. 12}]$$

Where CC is crown cover of species i and j; SF is sap flow of species i and j and A is the area of the catchment. Crown cover is calculated as the total number of crowns times the average canopy area of all crowns.

The use of a simple average value for canopy area may be not adequate if the range of canopy sizes is large (Čermák et al., 2004). This is the case in the Sardón catchment (Figure 10), where the difference between the mean and the median values of canopy area are 46.02 m² for *Q. Ilex* and 55.60 m² for *Q. Pyrenaica*. Therefore, canopy areas have been divided into four size classes with a statistical technique based on the quartiles of total canopy area.



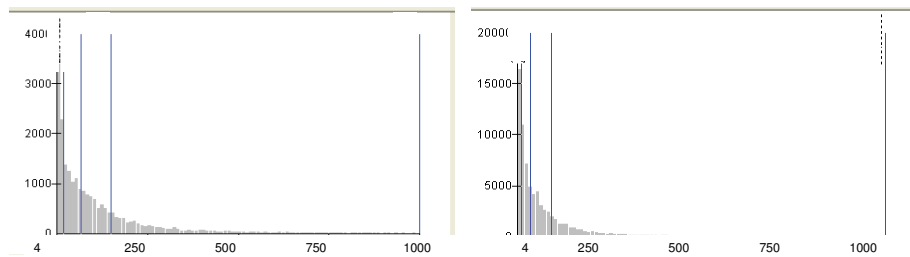


Figure 8 Canopy sizes and their frequency distribution in the Sardón catchment. Quartiles are shown in blue vertical lines.

All values of canopy area (separated by species) were sorted in an ascending manner and cumulative. Then, canopies smaller than 4 m² and bigger than 1000 m² were filtered out of the analysis; they usually represent pruned trees or shrubs and trees that grow very close to each other (and thus were not be separated by segmentation).

The total value of canopy area was divided into four equal portions delimited by the quartiles, rounded up to the next integer. The mean value of each class was finally multiplied by the number of trees in that class (in order to obtain the crown cover) and then multiplied again by the sap flow value of one of the sampled trees (Table 2) in the corresponding class.

2.5.3.2 Upscaling based on the Penman-Monteith model

Methods to estimate catchment-level transpiration directly have not been applied as widely as the methods described in the previous subchapters. There are still uncertainties about appropriate scalars for transpiration at the catchment level. At this spatial scale, transpiration is generally estimated with a “top-down” approach using remote sensing products to calculate the surface energy balance. Transpiration is usually estimated as a residual of the energy balance.

Table 4 mentions the use of Radiative Transfer Models (RTM) for upscaling transpiration at all spatial scales. Although their potential for modelling transpiration (and also other physiological processes such as carbon assimilation and fluorescence) has been proved, their implementation in analysis at the catchment

level is still a challenge given the current average computational capacities. Other potential difficulties for their regional application include the definition of input slopes and altitudes, which influence radiation interception.

Čermák et al. (2004) suggest the use of “scaling curves”, both at the stand and catchment level. Transpiration values of sampled trees and biometric or spectral characteristics that can be observed in a satellite image, for example near-infra red or thermal reflectance, might prove to be related (Čermák et al. found non-linear relations between transpiration and DBH), but given the limited number of transpiration samples, this method would not give a reliable estimation for the Sardón catchment.

It was decided therefore to take a similar approach as the one taken for stand upscaling, under the assumption that if a tree can be represented as a single “big leaf”, then a catchment can be treated as a “big stand”. The surface temperature of each species was calculated as the product of the sunlit/shaded canopy area by the measured leaf temperatures (similarly to Equation 11). Canopy conductance was calculated with Equation 8 and all the other variables were derived from averages of meteorological data for the period 11:30 am – 14:30 pm for the days 15th to 17th September, 2009. Finally, the sum of transpiration values of *Q. Ilex* and *Q. Pyrenaica* for each day was divided by the catchment area to obtain the total transpiration.

3. Results and Discussion

3.1. Tree species classification and mapping

Intermediate and final outputs of the two classification procedures performed are shown in Figures 8 and 9.

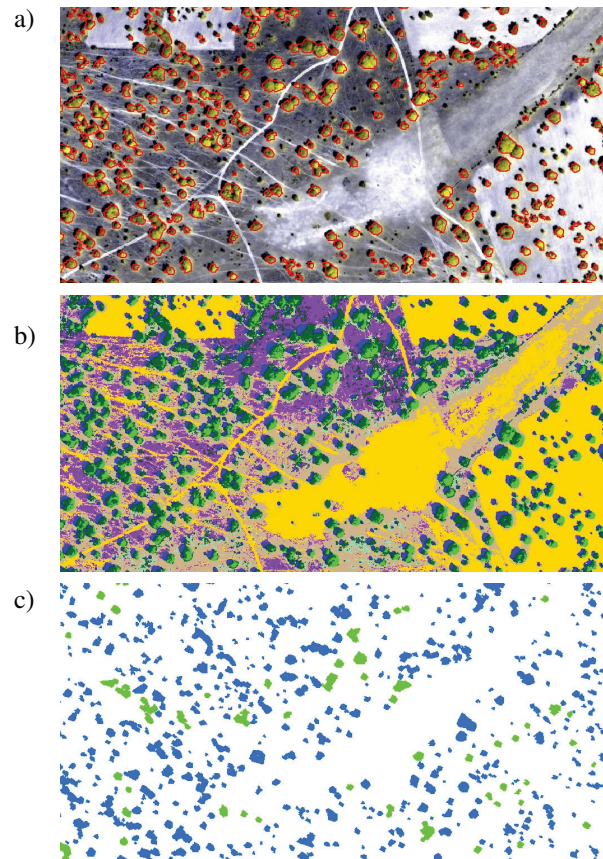


Figure 9 Spectral classification with object-oriented analysis

a) Individual trees (with red outline) separated from the background after segmentation. b) Preliminary supervised species classification, showing pixels classified as *Q. Ilex* in dark green, *Q. Pyrenaica* in light green, shadows in blue and other land cover classes in yellow, purple, cyan and grey. c) Final species classification after object-oriented and spectral analysis: *Q. Ilex* in blue and *Q. Pyrenaica* in green.

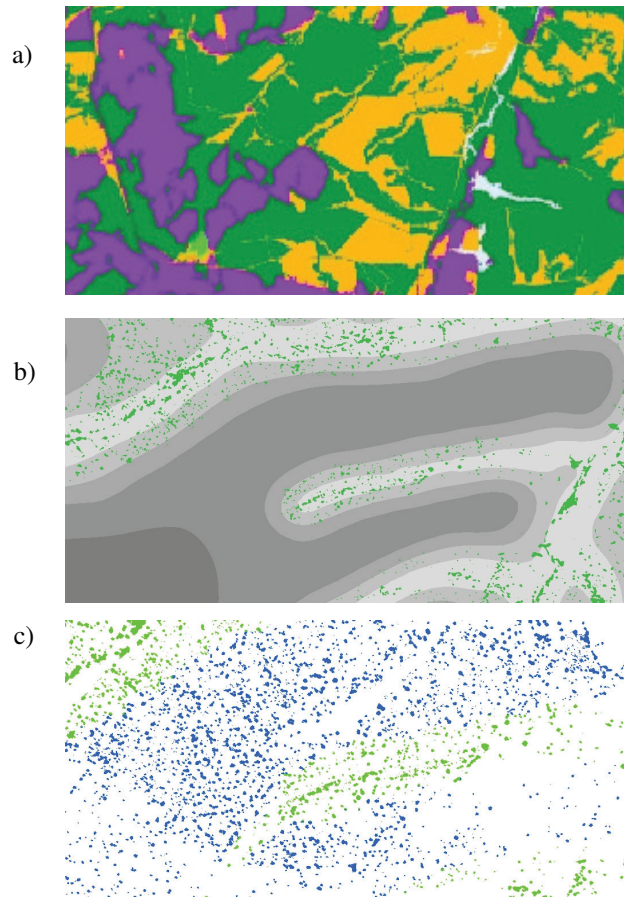


Figure 10 Multi-criteria classification results

a) Physiographic units of part of the Sardón catchment. Only the rocky areas (in purple) were used for tree classification. b) Groundwater depth in shades of grey and preliminary classification of trees as *Q. Pyrenaica* in areas of shallow water table. c) Final species classification after multi-criteria evaluation: *Q. Ilex* in blue and *Q. Pyrenaica* in green.

Table 5 shows the accuracy assessment performed for the tree species classification. The method based on spectral and object-oriented approaches (“Spectral Method”) yielded a classification with an overall accuracy of 80%, whereas the method based on field observations and expert knowledge (Multi-criteria, “M.C. Method”) reached 79%. Because the accuracy assessment relies on

sample locations where tree species were identified, it is not possible to calculate it exactly. Nevertheless, a z test (Table 6) showed that the true map accuracy is located between 75% and 84% for the Spectral Method and between 74% and 83% for the M.C. Method. It has been possible to estimate these accuracies with a small confidence interval given the large amount of field points collected.

It is important to mention that this sample collection has not followed any statistical sampling design, as the species identification points are part of a multi-purpose dataset available to several researchers. On the other hand, a random sampling design for point collection would have probably included many unrepresentative points, as certain areas of the catchment have predominantly one tree species, and random distribution is observed in only some areas (M.C. Method has used non-random criteria of tree distribution). Moreover, the fact that there is more than double amount of sample points for *Q. Ilex* could lead us to think about an overrepresentation of correctly mapped trees (the so-called Type II error: accepting an incorrect map), but it actually represents the proportion of species in the sampled area.

Table 5 Error matrices for accuracy assessment. Based on (Pilesjo, 2009)

SPECTRAL METHOD					M.C. METHOD						
		FIELD DATA					FIELD DATA				
Map Data		Ilex	PYR	Total	Map Data		Ilex	PYR	Total		
		Ilex	225	51		276		Ilex	230	58	288
		PYR.	12	22		34		PYR	7	15	22
		Total	237	73		310		Total	237	73	310

	Ilex	PYR
A	225	22
B	237	73
C	276	34
N	310	310

	Ilex	PYR	
A	230	15	correct points
B	237	73	field points
C	228	22	map data points
N	310	310	total points

Overall Accuracy 0.80

Probability that a randomly chosen point (from map or field) is correctly mapped

User Accuracy

Ilex 0.82
PYR 0.65

Probability that a randomly chosen point on the map has the same class in the field

Producer Accuracy

ILEX 0.95
PYR. 0.30

Overall Accuracy 0.79

User Accuracy

ILEX 0.799
PYR 0.682

Producer Accuracy

ILEX 0.970
PYR. 0.205

Probability that a randomly chosen point in the field has the same class in the map

Table 6 z test to define confidence intervals

Statistics	Spectral	M.C.
n	310	310
correctly classified	247	245
p	0.796774	0.7903226
Standard Error	0.022855	0.0231205
confidence level	95%	95%
z	1.96	1.96
confidence interval	0.751979 0.841569	0.7450064 0.8356388

Kappa statistics have also been calculated to estimate the influence of chance in the classification (Table 6). The Spectral method outperforms the Multi-criteria method, as evidenced by a higher Kappa value. As there are two classes (species) in the map, there is the probability that 50% of trees are correctly classified, only by chance. The values of Kappa represent an improvement in the classification (Figure 11). In the case of the Spectral Method, this means that if 50% of samples (155 trees) were correctly classified only by chance, the classification by this method presents 30.8% more trees correctly classified in the sample (that is 95 trees). The M.C. Method presents 23.2% (71 trees). For this reason, it was decided to use the classification obtained by the Spectral Method for transpiration upscaling. Otherwise, the McNemar's test proved that the same proportion of trees would be correctly classified by the Spectral and the M.C. Methods (Table 7).

Table 7 Kappa statistics for the two classification methods

SPECTRAL METHOD				M.C. METHOD			
	Total	ILEX	PYR		Total	ILEX	PYR.
N	310	237	73	N	310	237	73
d	247	225	22	d	245	230	15
q	67894	65412	2482	q	69862	68256	1606
Kappa	0.308			Kappa	0.232		

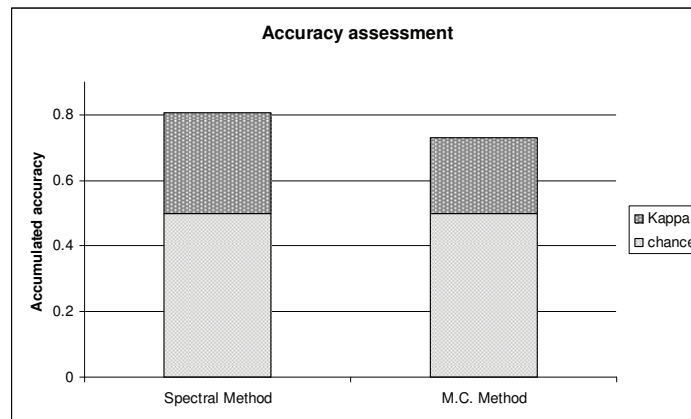


Figure 11 Graphical explanation of map accuracy.

Table 8 McNemar's test for dependent samples

Ho: The same population proportion of trees will be correctly classified by the Spectral and the M.C. methods.
H1: A different population proportion of trees will be correctly classified by the Spectral and the M.C. methods.

	M.C. Method			
	wrong	correct	total	
Spectral Method	wrong	45	21	66
	correct	14	230	244
	total	59	251	310

sample ratio = 1.5
 chi sq χ^2 = 1.4
 χ^2 table ($p = 0.25$; 1 degree of freedom) 1.32
 χ^2 table ($p = 0.90$; 1 degree of freedom) 2.71

If $\chi^2 >$ tabulated value, reject Ho, otherwise, do not reject Ho

We fail to reject Ho. The Spectral method and the Multi-criteria method have similar classification performance.

With respect to the M.C. Method, it is important to mention that the criteria used were conceived as “hard” classifiers, Boolean-type criteria, whereby a region was excluded from the analysis if it failed to meet an arbitrary threshold (e.g. *Q. Pyrenaica* trees classified as *Q. Ilex* if located outside river banks). The criteria were also weighted equally in the final combination; a different weighted combination of

criteria could have yielded either an improved or a worse classification. According to the results presented in this chapter, the criterion that might deserve more weight is the spectral information.

The application of fuzzy set memberships to the used criteria (procedure iii in Chapter 2.2; not tested) could be another option to enhance the M.C. Method, as it provides a stronger logic for the process of criteria standardization than Weighted Linear Combination (Jiang and Eastman, 2000).

3.2. Transpiration upscaling to tree level

Following the procedures described in Chapter 2.3, and using field measurements of xylem length (2 cm of xylem length), mean transpiration for the sample trees of the Sardón catchment was calculated. The results are presented in Table 8.

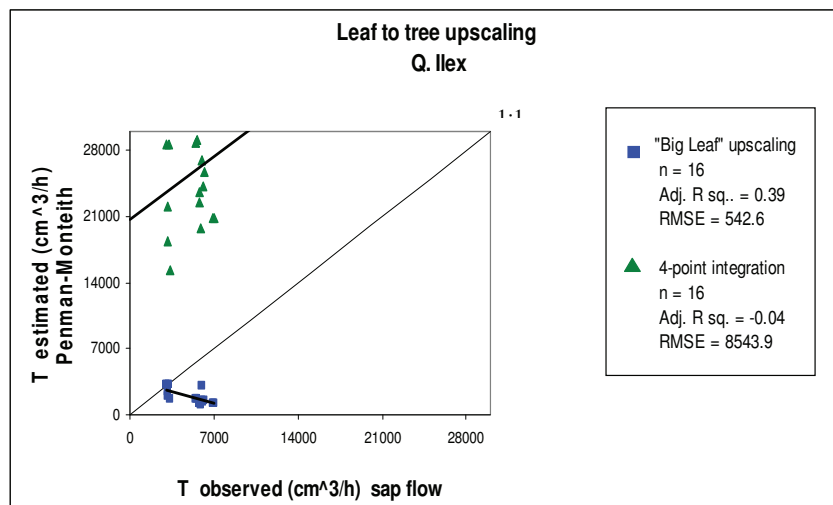
Table 9 Calculation of mean transpiration for a single tree from sap flow measurements

Name of tree	Dates	Sap flux density	DBH	Xylem length	Sapwood area	Sap Flow
		cm ³ /cm ² /h	cm	cm	cm ²	cm ³ /h
Ilex1 (GR)	15 – 17 Sept. 2009	10.12	27	12	376.99	3815.16
Ilex2 (HFD)	15 – 17 Sept. 2009	3.48	57	5.4	452.11	1573.34
Ilex3 (HFD)	2 - 4 Sept. 2009	3.95	32.50	11	449.25	1774.53
PYR1 (GR)	15 – 17 Sept. 2009	12.84	16.50	3.90	79.95	1026.51
PYR2 (HFD)	11 – 13 Sept. 2009	3.71	43.00	7.50	444.73	1787.83

PYR3 (GR)	18 – 20 Aug. 2009	8.57	36.50	15.20	654.21	5606.284
-----------	----------------------	------	-------	-------	--------	----------

The instantaneous transpiration rates upscaled from leaf-level measurements were compared to corresponding tree sap flow rates of transpiration (Figure 12). The integration of LAI over the height of the canopy (Gaussian integration method) proved to be a reasonable estimator of tree transpiration for *Q. Pyrenaica*, with a mean difference of 10.5% with the sap flow rates (Figure 13). Nevertheless, for *Q. Ilex*, the mean difference between calculated and observed transpiration rates is more than 100%. The “big leaf” (Dingman, 2002) upscaling approach (that is, multiplying the sap flow rate by the ratio of canopy area and LAI) resulted in mean differences of 36% for *Q. Pyrenaica* and 55% for *Q. Ilex*, respectively. There are several reasons that explain these results.

First, the better performance in *Q. Ilex* might be due to the similarity of the transpiration estimations, i.e. the multiplication of a measured parameter by the sapwood or leaf area of the tree.



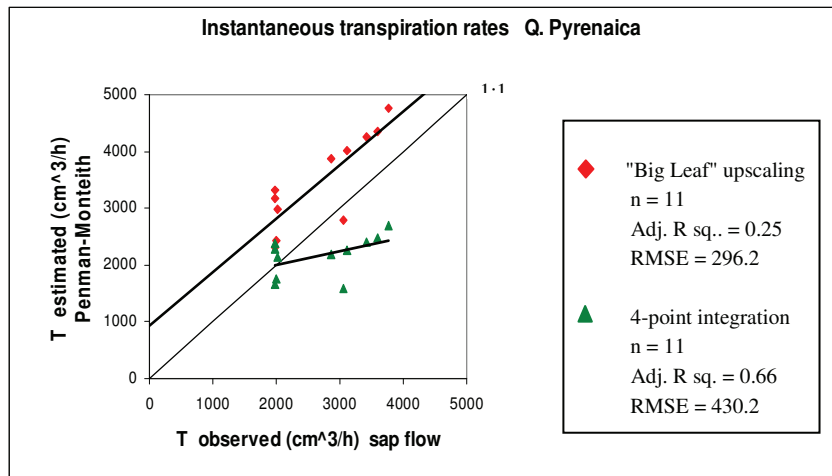


Figure 12 Regression for sap flow-based transpiration at the tree level against estimations derived from the “big leaf” approach (T^*CA/LAI) and Gaussian integration method (T^*LAI).

Table 10 t test to prove agreement between Penman-Monteith and “Big Leaf” model.

H0 = There is no difference between upscaled values using canopy area and integrated LAI						
H1 = There is difference between upscaled values using canopy area and an integrated LAI						
	Q. Ilex		Q. Pyrenaica			
	<i>T rate SF</i>	<i>T*(CA/LAI)</i>	<i>T rate SF</i>	<i>T*(CA/LAI)</i>	<i>T rate SF</i>	<i>T*LAI</i>
Mean	5179.362	1831.742	2710.26	3474.839	2710.26	2163.889
Variance	2087944	516949.8	528012.5	674602.3	528012.5	128701.4
Observations	16	16	11	11	11	11
Pooled Variance	1302447		601307.4		328356.9	
Degrees of freedom	30		20		20	
t Stat	8.296619		-2.31236		2.236125	
P(T<=t) two-tail	2.92E-09		0.031529		0.036901	
t Critical two-tail	2.042272		2.085963		2.085963	
alpha	0.05		0.05		0.05	

Reject Ho!

Reject Ho!

Reject Ho!

Reject Ho!

Upscaled transpiration values are significantly different from sap flow measurements

Secondly, the results might reflect a bigger variation of LAI values along the height of the canopy in *Q. Ilex*, which could have been not represented by the measurements of LAI at four heights.

Ansley, Dugas et al.(1994) remark that “transpiration measured by a porometer and scaled to the stem or canopy is greater than the measured by stem flow or gravimetric techniques, especially during periods of high transpiration”. In the Sardón catchment, this is the case for *Q. Pyrenaica*, but not for *Q. Ilex*. It is important to mention that there was a significant amount of noise in the *Q. Ilex* data, arisen from the fact that the small leaves of this species do not fill the leaf chamber completely (Figure 12).

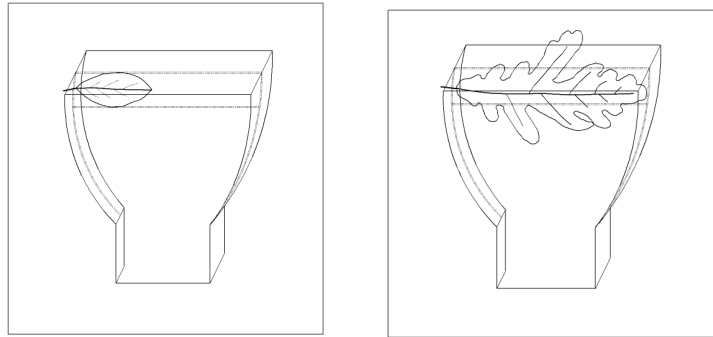


Figure 13 Schematic representation of the leaf chamber with leaves of *Q. Ilex* (left) and *Q. Pyrenaica* (right). The leaf chamber has a measurement area of 6.5 cm^2 ; *Q. Ilex* leaves are about 3 cm^2 and *Q. Pyrenaica* leaves about 25 cm^2 .

An important consideration is that sap flow data have been taken as the observed values for comparison. Actually, there are also uncertainties related to the values of sap flow that can help in the explanation of the results. As mentioned in Chapter 2.3, data from the outer 2 cm of sapwood have been used for transpiration calculations, despite the fact that *Q. Ilex* conducts more sap in the internal part of the xylem. The contrary is valid for *Q. Pyrenaica* (Figure 14). Further, it is believed that when phreatophyte tree species like *Q. Ilex* pump groundwater, it is transported only through the internal part of the sapwood (Čermák et al., 2008).



Figure 14 Representation of the magnitude of sap flux density along the radius of the sapwood for *Q. Pyrenaica* (left) and *Q. Ilex* (right).

An interesting finding from the poor agreement between compared methods is that, contrary to the initial assumption, the analyzed species store water in the stem. This is why the magnitude of transpiration estimations based on measurements at the canopy is different from transpiration estimations based on measurements at the stem. Stem water storage has been identified to be an adaptation to drought periods and “the relative contribution of trunk water storage to transpiration depends on climatic demand and soil water depletion, as well as on tree age” (Hernández-Santana et al., 2008).

Although neither of the two approaches proved to yield significantly similar transpiration rates to the sap flow rates (at 0.05 significance level, see Table 10), better results were expected for the upscaling with integrated LAI, being it a more detailed description of the canopy. Apparently, the use of several LAI values introduced errors the calculation. The simple division of the canopy in layers, without any specification of the radiation interception will not yield better estimates than the generalized upscaling using one value of leaf area. Figure 13 shows leaf temperature values for the sunlit and shaded portions of the canopy, collected at the same time of transpiration measurement and with the same CI-340 instrument. Values are significantly different (at 0.05 significance level) for *Q. Ilex*, but not for *Q. Pyrenaica*, which might partially explain the results obtained.

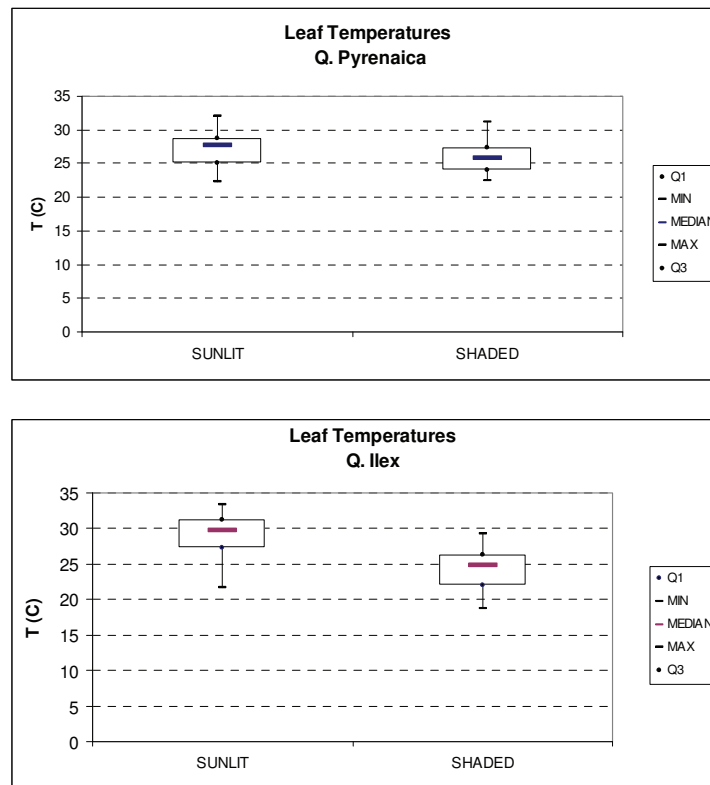


Figure 15 Leaf temperatures for 12 samples of *Q. ilex* and 15 samples of *Q. Pyrenaica*.

3.3. Transpiration upscaling to stand level

Transpiration rates estimated by sap flow measurements were upscaled using canopy area values and Equation 6. The Biometric Upscaling Functions in Figure 8 demonstrate that there is a good correlation between canopy and sapwood area both for *Q. ilex* and for *Q. Pyrenaica*, with more dispersion at higher values of canopy area.

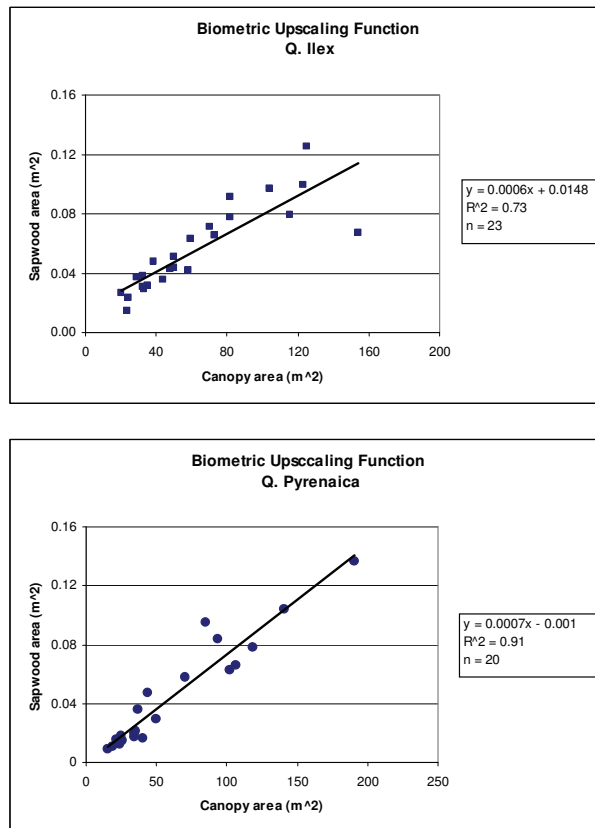


Figure 16 Biometric Upscaling Functions

For the 1 ha stand shown in Figure 8, the total transpiration rate at midday hours of clear days was 0.006 mm/h. The calculation was repeated using sapwood area as scalar. The difference in hourly transpiration equals $1 \cdot 10^{-4}$ mm, which can be attributed to systematic errors. The results confirm the suitability of the Biometric Upscaling Functions for the estimation of biometric parameters and sap flow upscaling. It is important to mention that the data used for upscaling was obtained during the 11:30 am – 14:30 pm period, which represents the maximum daily values of transpiration.

Table 11 Results of transpiration upscaling at the stand level using sap flow measurements
 SFs = sample sap flow; CAs = sample canopy area; CA_t = total canopy area; SAs = sample sapwood area; SA_t = total sapwood area; T = transpiration

ILEX			PYRENAICA			TOTAL		
SFs	0.004	m ³ /h	SFs	0.006	m ³ /h	T	0.0718	m ³ /h
CAs	100.940	m ²	CAs	63.115	m ²	T	0.0071	mm/h
CA _t	669.119	m ²	CA _t	582.530	m ²			
T	0.0252	m ³ /h	T	0.0517	m ³ /h			

SFs	0.004	m ³ /h	SFs	0.006	m ³ /h	T	0.0778	m ³ /h
SAs	0.075	m ²	SAs	0.043	m ²	T	0.0077	mm/h
SA _t	0.579	m ²	SA _t	0.401	m ²			
T	0.02931	m ³ /h	T	0.0520	m ³ /h	Stand total		
						0.0148	mm/h	

In the previous sub-chapter it was demonstrated that a characterization of the radiation inside the canopies is necessary to estimate transpiration accurately using the Penman-Monteith model. At the stand level, the differences in temperature within the canopies were considered, resulting in a stand transpiration of 0.0138 mm/h, which almost coincides with the sap flow-based transpiration estimate and with sap flow transpiration estimates for September 2001 and 2003 reported by Lubczynski and Gurwin (2005) in the Sardón catchment. The good agreement of the estimations can be attributed to the similar nature of the sample measurements, which are based on temperature differences inside the trunk and within the canopy. The results also highlight the importance of radiation in the transpiration process of the Sardón catchment.

3.4. Transpiration upscaling to catchment level

The total transpiration rate of the Sardón catchment was estimated using instantaneous measurements of sap flux density for two trees of each species and the mean canopy area of each crown-size class. Sap flux density values represent the sap movement in the outer 2 cm of sapwood area. The total transpiration of all *Q. Pyrenaica* trees is 12.5 mm/h and 39.3 mm/h for all *Q. Ilex* (Figure 13). These are transpiration rates corresponding to 11:30 – 14:30 hours of the 15th to 17th

September, 2009. At these hours of the day sap flow rates reach their maximum values.

Table 12 Calculation of total tree transpiration in the Sardón catchment using the quartiles (Q) of canopy area distribution.

Q. ILEX					
	Q1	Q2	Q3	Q4	Total
	16	40	100	1000	
Mean canopy area (m ²)	11.1	28.11	65.09	248.97	
St. Dev.	2.65	6.73	16.92	180.24	
Frequency	19159	17992	20092	18338	
Mean sapwood area (m ²)	0.02146	0.031666	0.053854	0.164182	
Reference tree	Ilex1	Ilex3	Ilex3	Ilex2	
Sap flux dens. (m ³ /m ² /h)	0.1012	0.0395	0.0395	0.0348	
Sap flow (m ³ /h)	0.0021	0.0012	0.0021	0.0057	
Crown cover	376.18	158.18	61.17	17.52	
T (m ³ /h)	0.82	0.20	0.13	0.10	1.25
T (mm/h)					0.12
Q. PYRENAICA					
	Q1	Q2	Q3	Q4	Total
	22.61	69.21	152.51	995.48	
	23	70	152	1000	
Mean canopy area (m ²)	13.4	44.44	105.66	333.07	
St. Dev.	4.56	13.64	23.2	192.96	
Frequency	5613	5414	5375	5458	
Mean sapwood area (m ²)	0.008	0.030	0.073	0.232	
Reference tree	Pyr1	Pyr1	Pyr3	Pyr2	
Sap flux dens. (m ³ /m ² /h)	0.1284	0.1284	0.0857	0.0371	
Sap flow (m ³ /h)	0.001	0.004	0.006	0.009	
Crown cover	1,063.63	332.50	140.86	44.01	
T (m ³ /h)	1.14	1.29	0.88	0.38	3.69
T (mm/h)					0.37

Total catchment transpiration (mm/h)		0.49
--------------------------------------	--	-------------

It is possible that the modelling of tree transpiration in the smaller and bigger canopy area classes may have suffered misestimation, as the samples of sap flux density were taken only in mid-aged, healthy trees with a uniform, straight trunk.

The results of the Penman-Monteith estimation of transpiration are presented in Table 13. The reasons for non-agreement explained in Chapter 3.2 apply also to catchment level, notably the underestimation of *Q. Ilex* transpiration due to the use of data of the outer 2 cm of sapwood.

Table 13 Important variables and results of the Penman-Monteith calculations at the catchment level. Definitions and formulas are given in Chapter 2.4.

Day	Species	ΔTemp	L	e_a	g_{can}	K	T
Date	Name	Kelvin	W/m^2	Pa	m/s	Unitless	mm/h
15/09/2009	Q. Ilex	11.462	179.002	1.856	0.226	7.44067 E-06	0.15817
15/09/2009	Q. Pyrenaica	10.016	179.002	1.856	0.412	7.44067 E-06	0.04755
16/09/2009	Q. Ilex	12.194	179.002	1.771	0.075	7.46723 E-06	0.47556
16/09/2009	Pyrenaica	10.748	179.002	1.771	0.137	7.46723 E-06	0.14299
17/09/2009	Q. Ilex	13.135	179.002	1.667	0.126	7.46561 E-06	0.2826
17/09/2009	Pyrenaica	11.688	179.002	1.667	0.230	7.46561 E-06	0.085
Total							1.1919
Total m^3/h							11.919

3.5. Considerations on sources of error

Canopy area and Leaf Area Index (LAI) have been used throughout this study to upscale tree transpiration. It is therefore necessary to consider the uncertainties

related to the generation of these scalars, both in the field and with the aid of remote sensing.

The segmentation of tree canopies obtained by object-oriented analysis is very satisfactory but still not perfect in all areas of the Sardón catchment. Trees that grow too close together have been segmented sometimes as one tree (Figure 8). This generally does not have a negative influence on transpiration at the tree level, because the transpiration from a “double tree” is equal to the sum of the transpiration for two separate trees. Nevertheless, for upscaling purposes, the Biometric Upscaling Functions may not work as well with “groups” of trees. That is specially the case if the trees have different stem diameter. Segmenting the image to a finer scale (and probably using another algorithm) could maybe have enhanced the canopy delineation, but it is time- and computational expensive. Moreover, the identification of individual trees in dense forest stands is still a challenge in object-oriented analysis (Chavarro, 2009).

Another factor influencing the variability of canopy area in the Sardón catchment is the management of agricultural land. It was observed during fieldwork that cattle eat tree branches and reshape the lower part of the canopies (Figure 14). Also, many pruned trees were to be found, which is a normal pattern in the region. “Several prunings are done during the life of the oaks (...), the aim is to maximize acorn production” (Joffre et al., 1999). Oak acorns are the principal food for the high-value Iberian pig. For this reason, a truly representative tree sampling in the area is difficult to obtain, and transpiration estimations based on canopy area are highly variable.



Figure 17 A canopy of *Q. Pyrenaica* modified by pruning and by cattle.

Because pruning increases the area of empty spaces within the canopy, thus making it permeable to heat fluxes from the ground, radiation-based estimations of transpiration are subject to inaccuracies. For example, canopy temperature can be retrieved from thermal remote sensing products. To date, the spatial resolution of thermal imagery is not lower than 90 by 90 meters. That means that pixels have a mixture of soil and canopy thermal radiance, not always easy to separate, especially if pruned trees are present.

4. Conclusions

Recalling the research questions made in Chapter 1.3, and evaluating the results presented in Chapter 3, the following conclusions were drawn:

Object-oriented analysis of high-resolution satellite images contribute significantly to the accuracy of transpiration estimations by supporting pixel-based land cover classifications and radiation analysis at the canopy level. The *Quercus* species present in the Sardón area are difficult to identify spectrally during the dry season (Figure 3), hence species identification relied on semantic properties of each tree, defined as an object. In the same way, the radiation distribution of individual canopies could be assessed for a large area with an object-oriented approach in order to scale up transpiration as a function of temperature.

Upscaling is a convenient method to include in the otherwise complex water balance solution of Water Limited Environments. Despite the ease of implementation, care has to be taken in the selection of a sampling method and suitable scalars. The selection of an upscaling method for tree transpiration depends on the purpose of the study or project, from which a sampling scheme, required accuracy and available resources will be decided upon. Transpiration is species-specific, and also site-specific. In the Sardón catchment, sapwood area and canopy area proved to be good estimators of tree transpiration (Table 9), but no general rules can be concluded, as plants tend to adapt to different environmental conditions by anatomical modifications.

The correct characterization of the variation of biometric parameters used in the upscaling process is fundamental for the accurate estimation of tree transpiration, especially at larger spatial scales (Figure 10). For this reason, field measurements are important control data. Also, the increasing accuracy of remote sensing techniques (for example the use of radar to estimate tree height) will improve the estimations in the near future.

The “Big Leaf” model is an upscaling method that is easy to implement and gives acceptable results. Nevertheless, many assumptions are made when using it and as a result, the upscaling results might be difficult to interpret if there is no previous knowledge about the species studied and the environmental conditions. If this knowledge is available, then certain improvements can be made to the model; for example, surface temperature specifications, like the one demonstrated in Chapters 2.5.2.2 and 3.3.

5. References

- Abrahams, A. D. and A. J. Parsons (1994). Geomorphology of deserts environments A. D. Abrahams and A. J. Parsons. London, New York, Chapman & Hall: 1 - 12.
- Abtew, W. and J. Obeysekera (1994). "Lysimeter Study of Evapotranspiration of Cattails and Comparison of three Estimation Methods." Transactions of the American society of Agricultural Engineers ASAE **1**: 121-129.
- Agbakpe, B. (2010). Estimating tree groundwater transpiration in La Mata Catchment, Spain. Water Resources Department. Enschede, University of Twente. **MSc Thesis**.
- Allen, R. G., L. S. Pereira, et al. (1998). Crop evapotranspiration - Guidelines for computing crop water requirements - FAO Irrigation and drainage paper 56. Rome, FAO - Food and Agriculture Organization of the United Nations.
- Ansley, R. J., W. A. Dugas, et al. (1994). "Stem flow and porometer measurements of transpiration from honey mesquite (*Prosopis glandulosa*)." Journal of Experimental Botany **45**(275): 847-856.
- Bastiaanssen, W. G. M., E. J. M. Noordman, et al. (2005). "SEBAL Model with Remotely Sensed Data to Improve Water-Resources Management under Actual Field Conditions." Journal of Irrigation and Drainage Engineering **131**(1): 85 - 93.
- Bowes, C., D. Unger, et al. (2007). Using Remotely Sensed Data to Quantify Contaminated Brine Sites in Southwest Texas. 21st Biennial Workshop on Aerial Photography, Videography, and High Resolution Digital Imagery for Resource Assessment. Terre Haute, Indiana.
- Čermák, J., J. Kučera, et al. (2004). "Sap flow measurements with some thermodynamic methods, flow integration within trees and scaling up from sample trees to entire forest stands." Trees **18**: 529–546.
- Čermák, J., N. Nadezhdina, et al. (2008). "Scots pine root distribution derived from radial sap flow patterns in stems of large leaning trees." Plant Soil(305): 61 - 75.
- Chavarro-Rincon, D. (2009). Tree transpiration mapping from upscaled sap flow in the Botswana Kalahari. Enschede, ITC. **PhD Thesis**.
- Chavarro, D. (2009). personal communication. Enschede.
- CID, I. (2003). CI-340/CI-510 Ver. 5. Camas, Washington, USA.
- Cienciala, E., J. Kucˇera, et al. (2000). "Tree sap flow and stand transpiration of two Acacia mangium plantations in Sabah, Borneo." Journal of Hydrology **236**: 109–120.
- Congalton, R. G. (1991). "A Review of Assessing the Accuracy of Classifications of Remotely Sensed Data." Remote Sensing of Environment **37**: 35 - 46.
- Courault, D., B. Seguin, et al. (2005). "Review on estimation of evapotranspiration from remote sensing data: From empirical to numerical modeling approaches." Irrigation and Drainage Systems **19**: 223 - 249.
- Crosbie, R. S., B. Wilson, et al. (2007). "The upscaling of transpiration from individual trees to areal transpiration in tree belts." Plant Soil **305**: 25 - 34.
- David, T. S., M. O. Henriques, et al. (2007). "Water-use strategies in two co-occurring Mediterranean evergreen oaks: surviving the summer drought." Tree Physiology **27**: 793 - 803.

- de Leeuw, J., K. Schmidt, et al. (2002). McNemar's test for comparing the accuracy of categorical maps. Accuracy 2002: proceedings of the 5th international symposium on spatial accuracy assessment in natural resources and environmental sciences. G. Hunter and K. Lowell. Melbourne, Delft University Press.
- Definiens, A. (2007). Definiens Developer 7, Reference Book. Munich, Definiens AG.
- Dingman, S. L. (2002). Physical Hydrology. Upper Sadle River, Prentice Hall.
- Droogers, P. (2000). "Estimating actual evapotranspiration using a detailed agro-hydrological model " Journal of Hydrology **229**(1 - 2): 50 - 58.
- EARS. (2009). "Actual evapotranspiration field: 1 - 10 August 2009 " Retrieved 15/08, 2009, from http://www.ears.nl/evapotranspiration_field.php.
- Eastman, J. R. (2006). IDRISI Andes. Guide to GIS and Image Processing. Worcester, USA, Clark Labs, Clark University.
- Ford, C. R., R. M. Hubbard, et al. (2007). "A comparison of sap flux-based evapotranspiration estimates with catchment-scale water balance." Agricultural and Forest Meteorology **145**: 176–185.
- Gastellu-Etchegorry, J. P., D. V., et al. (1996). "Modeling radiative transfer in heterogeneous 3-D vegetation canopies." Remote Sensing of Environment **58**: 131-156.
- Gieske, A. and W. Meijninger (2005). "High density NOAA time series of ET in the Gediz Basin, Turkey." Irrigation and Drainage Systems **19**: 285–299.
- Goudriaan, J. (1986). "A simple and fast numerical method for the computation of daily totals of canopy photosynthesis." Agricultural and Forest Meteorology **43**: 251-255.
- Granier, A. (1985). "Une nouvelle méthode pour la mesure du flux de sève brute dans le tronc des arbres " Annales des Sciences Forestières **42**: 193-200
- Habtemannian, T. B. (2000). Subsurface characterization of granitic basement from structural and resistivity data : a case study from Sardon catchment area, Salamanca, Spain. Enschede, ITC. **MSc**: 77.
- Hernández-Santana, V., T. S. David, et al. (2008). "Environmental and plant-based controls of water use in a Mediterranean oak stand." Forest Ecology and Management **255**: 3707-3715.
- Howel, T. A. and S. R. Evett (n.d.). The Penman-Monteith Method. Bushland, Texas, Conservation & Production Research Laboratory.
- Im, J. and J. R. Jensen (2005). "A change detection model based on neighborhood correlation image analysis and decision tree classification." Remote Sensing of Environment **99**(3): 326-340.
- Immerzeel, W. W., P. Droogers, et al. (2006). Remote Sensing and Evapotranspiration Mapping: State of the Art. Wageningen, International Water Management Institute.
- Infante, J. M., S. Rambal, et al. (1997). "Modelling transpiration in holm-oak Savannah: scaling up from the leaf to the tree scale." Agricultural and Forest Meteorology **87**: 273-289.
- Janssen, L., Huurneman, G.C., Bakker, W. Gorte, B., Reeves, C, Pohl, C., Weir, M., Horn, J., Prakash, A., Woldai, T. (2001). Principles of Remote Sensing. Enschede.
- Jiang, H. and J. R. Eastman (2000). "Application of fuzzy measures in multi-criteria evaluation in GIS." International Journal of Geographical Information Science **14**(2): 173 - 184.
- Joffre, R., S. Rambal, et al. (1999). "The dehesa system of southern Spain and Portugal as a natural ecosystem mimic." Agroforestry Systems **45**: 57 - 79.
- Kimani, J. (2004). Mapping od Dry Savannah Tree Species using Object-oriented Classification and High Resoulution Imagery in Serowe, Botswana, ITC. **MSc**: 94.
- Koestner, B. M. M., E. D. Schulze, et al. (1992). "Transpiration and canopy conductance in a pristine broad-leaved forest of *Nothofagus*: an analysis of xylem sap flow and eddy correlation measurements." Oecologia **91**: 350-359.

- Kropff, M. J. and H. H. van Laar, Eds. (1993). Modelling crop-weed interactions. Wallingford, CAB International.
- Laliberte, A. S., A. Rango, et al. (2004). "Object-oriented image analysis for mapping shrub encroachment from 1937 to 2003 in southern New Mexico." Remote Sensing of Environment **93**: 198–210.
- Lu, P., L. Urban, et al. (2004). "Granier's Thermal Dissipation Probe (TDP) Method for measuring sap flow in trees: theory and practice." Acta Botanica Sinica **46**(6): 631 - 645.
- Lubczynski, M. and J. Gurwin (2005). "Integration of various data sources for transient groundwater modeling with spatio-temporally variable fluxes—Sardon study case, Spain." Journal of Hydrology **306**: 71–96.
- Lubczynski, M. W. (2009). "The hydrogeological role of trees in water-limited environments." Hydrogeology Journal **17**: 247–259.
- Mapanda, W. (2003). Scaling - up tree transpiration of eastern Kalahari sandveld of Botswana using remote sensing and geographical information systems Enschede, ITC. **MSc Thesis**.
- McNemar, Q. (1947). "Note on the sampling error of the difference between correlated proportions or percentages." Psychometrika **12**: 153–157.
- Moran, M. S., R. L. Scott, et al. (2009). "Partitioning evapotranspiration in semiarid grassland and shrubland ecosystems using time series of soil surface temperature." Agricultural and Forest Meteorology **149**: 59 - 72.
- Nadezhdina, Čermák, et al. (1998). Heat field deformation method for sap flow measurements Measuring Sap Flow in Intact Plants Č. J. and N. N. Brno (Czech Republic) IUFRO Publications, Publishing House of Mendel University
- Nakamba, G. (2002). Estimating transpiration from sap flow measurements : a case study of Sardon catchment, Salamanca, Spain. Enschede, ITC: 48.
- NASA. (2009). "MOD 16 - Evapotranspiration." Retrieved 16/08, 2009, from http://modis.gsfc.nasa.gov/data/dataproduct/dataproducts.php?MOD_NUMBER=16.
- Ontiveros, R. (2009). Tree transpiration, a spatio-temporal approach in water limited environments - Sardon study case. Water Resources. Enschede, International Institute for Geo-information Science & Earth Observation (ITC). **MSc Thesis**: 65.
- Pilesjo, P. (2009). Map Accuracy Assessment. LUMA-GIS Lecture Notes. Lund, Lund University: 229 - 242.
- Poyatos, R., J. Cermak, et al. (2007). "Variation in the radial patterns of sap flux density in pubescent oak (*Quercus pubescens*) and its implications for tree and stand transpiration measurements." Tree Physiology **27**: 537–548.
- Reyes, L. (unpublished).
- Rwarinda, E. M. (1996). Hydrogeological investigation in Sardon catchment, a part of the lower Rio Tormes basin, Salamanca province, Spain. Enschede, ITC: 95.
- Rwasoka, D. T. (2010). Evapotranspiration in water limited environments: up-scaling from crown canopy to the eddy flux footprint. Water Resources Department. Enschede, University of Twente. **MSc Thesis**.
- Samaali, M., D. Courault, et al. (2007). "Analysis of a 3D boundary layer model at local scale: Validation on soybean surface radiative measurements." Atmospheric Research **85**: 183-198.
- Shakya, D. R. (2001). Spatial and Temporal Groundwater Modelling Integrated with RS and GIS. Water Resources Management. Enschede, ITC. **MSc Thesis**.
- Snyder, R. L., M. Orang, et al. (2005). "Simplified Estimation of Reference Evapotranspiration from Pan Evaporation Data in California." Journal of Irrigation and Drainage Engineering **131**: 249 - 253.

- Su, Z. (2002). "The Surface Energy Balance System (SEBS) for estimation of turbulent heat fluxes." Hydrology and Earth System Sciences **6**(1): 85 - 99.
- Van der Tol, C., A. J. Dolman, et al. (2007). "Topography induced spatial variations in diurnal cycles of assimilation and latent heat of Mediterranean forest." Biogeosciences **4**: 137–154.
- Van der Tol, C., W. Verhoef, et al. (2009). "An integrated model of soil-canopy spectral radiance observations, photosynthesis, fluorescence, temperature and energy balance." Biogeosciences Discussions **6**: 6025-6075.
- Verhoeff, A. (1997). "The effect of temperature differences between porometer head and leaf surface on stomatal conductance measurements." Plant, Cell and Environment **20**: 641-64.
- Walter, I. A., R. G. Allen, et al. (2005). The ASCE Standardized Reference Evapotranspiration Equation. R. G. Allen, I. A. Walter, R. Elliott et al, Environmental and Water Resources Institute of the American Society of Civil Engineers
- Yan, G., J. F. Mas, et al. (2006). "Comparison of pixel-based and object-oriented image classification approaches—a case study in a coal fire area, Wuda, Inner Mongolia, China." International Journal of Remote Sensing **27**(18): 4039–4055.